

# Velocity Force Curves, Laning, and Jamming for Oppositely Driven Disk Systems

C. Reichhardt<sup>a</sup> and C.J.O. Reichhardt<sup>\*a</sup>

Received Xth XXXXXXXXXXXX 20XX, Accepted Xth XXXXXXXXXXXX 20XX

First published on the web Xth XXXXXXXXXXXX 200X

DOI: 10.1039/b000000x

Using simulations we examine a two-dimensional disk system in which two disk species are driven in opposite directions. We measure the average velocity of one of the species versus the applied driving force and identify four phases as function of drive and disk density: a jammed state, a completely phase separated state, a continuously mixing phase, and a laning phase. The transitions between these phases are correlated with jumps in the velocity-force curves that are similar to the behavior observed at dynamical phase transitions in driven particle systems with quenched disorder such as vortices in type-II superconductors. In some cases the transitions between phases are associated with negative differential mobility in which the average absolute velocity of either species decreases with increasing drive. We also consider the situation where the drive is applied to only one species as well as systems in which both species are driven in the same direction with different drive amplitudes. Finally, we discuss how the transitions we observe could be related to absorbing phase transitions where a system in a phase separated or laning regime organizes to a state in which contacts between the disks no longer occur and dynamical fluctuations are lost.

## 1 Introduction

A wide variety of systems can be modeled as a collection of interacting particles that, when driven over a quenched substrate, exhibit depinning and dynamical transitions as a function of increasing driving force<sup>1</sup>. Such systems include vortices in type-II superconductors<sup>2–4</sup>, electron crystals<sup>5</sup>, driven colloidal systems<sup>6–10</sup>, and sliding friction<sup>11,12</sup>. At low drives these systems are in a pinned state where the velocity is zero, while above a critical driving force, the particles become depinned and slide. Within the moving states there can be different dynamical modes of motion such as a plastic phase with strong fluctuations in the particle positions and velocities<sup>1,2,4,6,7</sup>. At higher drives the system can organize to a dynamically ordered state such as a moving crystal<sup>2,3,13</sup> or moving smectic<sup>4,13–16</sup>. For particles driven over a periodic substrate, additional types of dynamic phases can appear such as soliton motion or one-dimensional (1D) to two-dimensional (2D) transitions, along with ordered and disordered flow phases<sup>1,8–12,17–19</sup>. The transitions between these different dynamical states are associated with cusps, jumps, or dips in the velocity force curves, as well as with global changes in the ordering of the particle configurations or the amount of dynamical fluctuations. In all these systems the pinning arises from quenched disorder that is fixed in space; however, there can also be cases where the pinning is not fixed but

can move in response to the driven particles. For example, if a number of particles that are not coupled to the external drive can block the motion of particles that are coupled to the external drive, the driven particles can move the blocking particles and over time rearrange them to create a new landscape or pattern<sup>20,21</sup>. A previously studied system that closely resembles this case is two species of interacting particles driven in opposite directions that exhibit a variety of dynamical behavior, including a transition to a laning state<sup>22–28</sup> where the particles separate into quasi one-dimensional chains of the same species, as well as regimes in which the particles mix and undergo disordered flow. Such phases have been observed in experiments on colloids moving in opposite directions<sup>29</sup> and dusty plasma systems<sup>30</sup>. This type of system can also exhibit pattern forming states<sup>25,26,31,32</sup> and jammed or clogged states<sup>25,33</sup>. Certain active matter systems have similar behavior, such as pedestrian flows that can be mimicked by particles moving in opposite directions<sup>34</sup>.

In this work we examine a two-dimensional system of disks in the absence of thermal fluctuations. Half the disks are driven in one direction and the other half in the opposite direction, and we measure the net velocity of one disk species along with the amount of six-fold ordering as a function of the driving force and disk density. Previous studies of laning transitions have generally focused on systems of colloids or particles with Yukawa interactions<sup>22,24</sup>. In our case the system is close to the hard disk limit and the density  $\phi$  is defined as the area covered by the disks. For  $\phi > 0.9$  the disks form a triangular solid or jammed state<sup>35</sup>. For  $\phi \geq 0.55$  we

<sup>(a)</sup> Theoretical Division, Los Alamos National Laboratory, Los Alamos, New Mexico 87545, USA. Fax: 1 505 606 0917; Tel: 1 505 665 1134; E-mail: [cjrx@lanl.gov](mailto:cjrx@lanl.gov)

find that the disks can organize into four possible dynamic phases: a jammed phase (I) where all the disks are in contact forming a triangular solid with zero net velocity; a fully phase separated state (II) where the disks organize into two bands with crystalline order moving in opposite directions and disk-disk collisions do not occur; a strongly fluctuating disordered phase (III) where disk collisions are continuously occurring and the system has liquid like features; and a laning state (IV) where the disks form a series of lanes, disk-disk collisions are absent, velocity fluctuations drop to zero, and the system has smectic properties. The transitions between these phases correlate with changes in the net velocity of either species as well as with changes in the disk ordering and the nature of the dynamic fluctuations. The mobility in the phase separated and laning states is high since the disks can move freely past one another without collisions, while the transition to the disordered phase is accompanied by a drop in the net velocity, leading to a region of negative differential mobility similar to that found in transitions from laminar flow to turbulent flow as a function of increasing drive in certain systems with quenched disorder<sup>17–19</sup>. For  $\phi < 0.55$  the system always organizes into a laning state where all disk collisions are lost. We also examine the situation where only one species is driven and show that the same four phases can arise in the high density limit. Here the jammed state consists of a drifting solid phase where the non-driven disks lock to the driven disks, while the phase separated and laning states are composed of assemblies of driven disks moving past stationary regions of non-driven disks. These phases can even occur when both species are driven in the same direction with different couplings to the external drive. We conjecture that some of these transitions fall into the class of absorbing phase transitions<sup>36</sup> when the system reaches a state where the disk collisions and fluctuations are completely lost, similar to the recently observed irreversible-reversible transitions in periodically sheared disk systems<sup>37</sup>.

## 2 Simulation

We model a 2D system of size  $L \times L$  with  $L = 36.0$  with periodic boundary conditions in the  $x$  and  $y$  directions containing  $N_d$  disks of radius  $R_d = 0.5$ . The disk-disk interaction is modeled as a repulsive harmonic spring. The overdamped equation of motion for a disk  $i$  is

$$\eta \frac{d\mathbf{R}_i}{dt} = \mathbf{F}_{dd}^i + \mathbf{F}_D^i. \quad (1)$$

The disk-disk interaction force is  $\mathbf{F}_{dd} = \sum_{i \neq j}^{N_d} k(2R_d - |\mathbf{r}_{ij}|)\Theta(2R_d - |\mathbf{r}_{ij}|)\hat{\mathbf{r}}_{ij}$ , where  $\mathbf{r}_{ij} = \mathbf{R}_i - \mathbf{R}_j$ ,  $\hat{\mathbf{r}}_{ij} = \mathbf{r}_{ij}/|\mathbf{r}_{ij}|$ , and  $\Theta$  is the Heaviside step function. The spring constant  $k = 60$ , and we find negligible changes in the dynamics for larger values of  $k$ . Each disk is subjected to an applied driving force

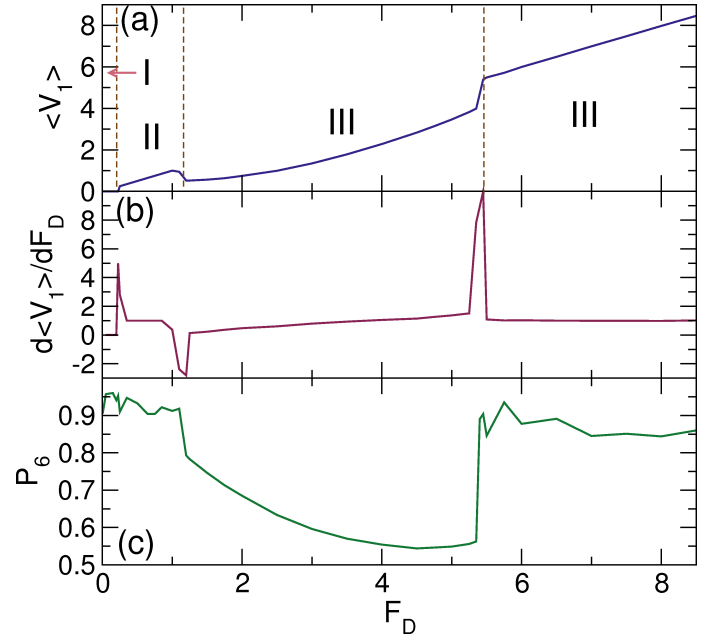


**Fig. 1** (a) The average velocity per disk  $\langle V_1 \rangle$ , measuring only the disks driven in the  $+x$  direction, vs  $F_D$  for a system with oppositely driven disks and  $N_1 = N_2 = 0.5N_d$  at  $\phi = 0.848$ . (b)  $d\langle V_1 \rangle/dF_D$  vs  $F_D$  for the same system. (c) The corresponding fraction of sixfold coordinated disks  $P_6$  vs  $F_D$ . We find four phases: I (jammed), II (phase separated), III (disordered flow), and IV (laning). The transitions between the states appear as jumps or dips in the various measures.

$\mathbf{F}_D^i = A^i F_D \hat{\mathbf{x}}$  where  $N_1$  disks are driven in the positive  $x$  direction with  $A^i = C$ , with  $C = 1.0$  unless otherwise noted. The remaining  $N_2 = N_d - N_1$  disks are driven in the negative  $x$  direction with  $A^i = -1.0$ . After applying the drive, we wait for the system to settle into a steady state. This transient waiting time is a strong function of disk density, and under some conditions can be as large as  $1 \times 10^8$  simulation time steps. After the system reaches a steady state we measure the average disk velocity for each species and normalize it by  $N_{1(2)}$  to obtain the average velocity per disk  $\langle V_{1(2)} \rangle = N_{1(2)}^{-1} \sum_{i=1}^{N_{1(2)}} \mathbf{v}_i \cdot \hat{\mathbf{x}}$ , where  $\mathbf{v}_i$  is the instantaneous velocity of disk  $i$ . Since we use overdamped dynamics with a damping constant of  $\eta = 1.0$ , in the free flow limit the disks move at a velocity of  $\langle V_1 \rangle = F_D$  and  $\langle V_2 \rangle = -F_D$ . The density  $\phi$  is defined as the area coverage of the disks,  $\phi = N_d \pi R_d^2 / L^2$ , and in the absence of driving the system forms a uniform crystalline solid at  $\phi = 0.9$ .

## 3 Velocity Force Curves and Dynamic Phases

We first consider samples in which  $N_1 = N_2 = 0.5N_d$ . In Fig. 1(a) we plot  $\langle V_1 \rangle$  versus  $F_D$  for the disks driven in the  $+x$  direction for a system with  $\phi = 0.848$ , and in Fig. 1(b) we

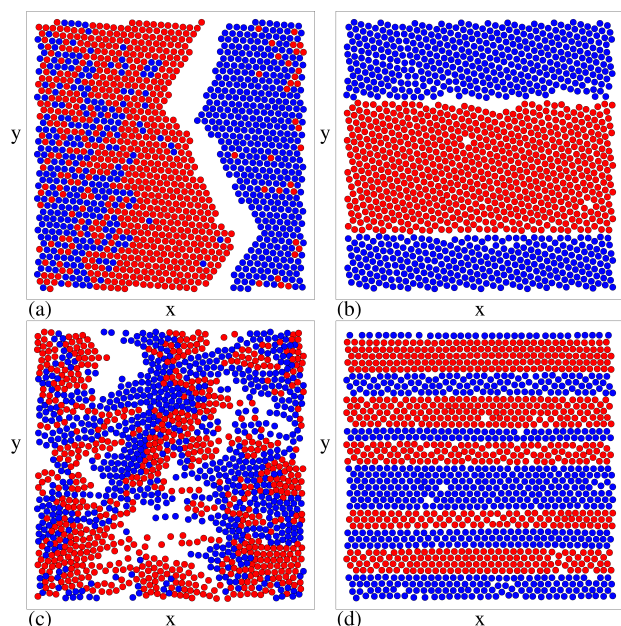


**Fig. 2** The disk configurations from the system in Fig. 1. The blue disks (species 1) are driven in the  $+x$  direction and the red disks (species 2) are driven in the  $-x$  direction. (a) The jammed phase I at  $F_D = 0.15$ . (b) The phase separated state II at  $F_D = 0.75$ . (c) The disordered phase III at  $F_D = 3.0$ . (d) The laning phase IV at  $F_D = 6.5$ .

show  $d\langle V_1 \rangle / dF_D$  versus  $F_D$ . We also measure the fraction  $P_6$  of sixfold coordinated disks for all disks,  $P_6 = \sum_i^{N_d} \delta(z_i - 6)$  where the coordination number  $z_i$  of disk  $i$  is obtained using a Voronoi construction, and plot  $P_6$  versus  $F_D$  in Fig. 1(c). The corresponding  $\langle V_2 \rangle$  versus  $F_D$  curve for disks driven in the  $-x$  direction looks exactly the same as the curve in Fig. 1(a) but is negative.

We identify four distinct dynamic phases based on transitions in the velocity-force curve. The jammed phase (I) appears for  $0 < F_D < 0.3$  and has no disk motion,  $\langle V_1 \rangle = 0$ , and strong sixfold disk ordering,  $P_6 \approx 0.95$ . In phase I, the disks form a dense cluster with triangular order, as illustrated in the disk configuration image in Fig. 2(a) for  $F_D = 0.15$ . Within the jammed phase the local disk density  $\phi_{\text{loc}}$  is close to  $\phi_{\text{loc}} = 0.9$ , and since this is lower than the total disk density, there is a small region containing no particles ( $\phi_{\text{loc}} = 0$ ). We note that in phase I  $P_6 < 1$  since the disks on the edge of the jammed cluster do not have six neighbors.

At  $F_D = 0.3$ , a jump in  $\langle V_1 \rangle$  and a peak in  $d\langle V_1 \rangle / dF_D$  indicate the transition from phase I to phase II, which is similar to the peak in  $d\langle V \rangle / dF_D$  observed in systems with quenched disorder at the pinned to sliding transition<sup>1</sup>. Phase II, the phase separated state, extends over the range  $0.3 < F_D < 1.15$ , and in this phase  $\langle V_1 \rangle$  increases linearly with increasing  $F_D$  and

$d\langle V_1 \rangle / F_D = 1.0$ , indicating that the particles are in a free flow regime. Additionally,  $P_6 \approx 0.92$  and both species exhibit triangular ordering as shown in Fig. 2(b) at  $F_D = 0.75$ .

At  $F_D = 1.15$  we find a transition from phase II to phase III accompanied by a drop in  $\langle V_1 \rangle$  which produces a negative spike in  $d\langle V_1 \rangle / dF_D$ . This is an example of negative differential mobility where the disk velocity decreases with increasing drive. The II-III transition is also associated with a drop in  $P_6$  when the system enters the disordered flow phase. In systems with quenched disorder, negative differential mobility has also been reported at transitions from ordered to disordered or turbulent flow phases<sup>11,17-19</sup>. Phase III appears for  $1.15 < F_D < 5.45$ , and is characterized by strongly fluctuating structures of the type shown in Fig. 2(c) for  $F_D = 3.0$ . The two particle species are strongly mixed and the sixfold ordering is lost. The disks continuously undergo collisions and show strong velocity deviations in the  $y$  direction, transverse to the drive. Within phase III,  $P_6$  gradually decreases to  $P_6 \approx 0.55$  near  $F_D = 5.45$ .

The transition from phase III to phase IV appears as an upward jump in both  $\langle V_1 \rangle$  and  $P_6$  along with a positive peak in  $d\langle V_1 \rangle / dF_D$ . As shown in Fig. 2(d) at  $F_D = 6.5$ , in phase IV the disks form multiple oppositely moving lanes. There is considerable triangular ordering of the disks within each lane which produces the increase in  $P_6$  at the III-IV transition. For higher values of  $F_D$ , the system maintains phase IV flow and  $d\langle V_1 \rangle / dF_D = 1.0$ , indicating that the disks are in a free flow regime.

We can characterize the structure of the disks in the different phases using the structure factor  $S(\mathbf{k}) = N_d^{-1} |\sum_i^{N_d} \exp(-i\mathbf{k} \cdot \mathbf{r}_i)|^2$ . In Fig. 3(a) we plot  $S(\mathbf{k})$  for the system in Fig. 2(a) in phase I at  $F_D = 0.75$ , where we find six peaks indicative of triangular ordering. In phase II, Fig. 3(b) shows a sixfold pattern of peaks with a small amount of smearing of the peaks. The disordered flow phase III in Fig. 3(c) has a ring pattern indicative of liquid ordering, while in Fig. 3(d), the laning phase IV has two strong peaks at  $k_x = 0.0$  and four weaker side peaks consistent with a moving smectic structure containing some local triangular ordering. The changes in  $P_6$  and  $S(\mathbf{k})$  from a liquid structure to a moving smectic signature as a function of increasing  $F_D$  are similar to the transitions observed for particles moving over quenched disorder such as vortices in type-II superconductors<sup>2,3,15,16</sup>.

We can get insight into the dynamic fluctuations of the different phases by examining the time series of the instantaneous velocity  $V_1(t)$  of species 1 disks in the different phases. In Fig. 4(a) we plot  $V_1$  versus time in phase I at  $F_D = 0.15$ . Initially  $V_1$  is in a fluctuating transient state indicating that the disks are moving, but at later times the system organizes into a jammed state with  $V_1 = 0$ . In phase III at  $F_D = 0.75$ , Fig. 4(b) shows that there are initially strong fluctuations in  $V_1$  but that at later times the system settles into a fluctuation-free flowing

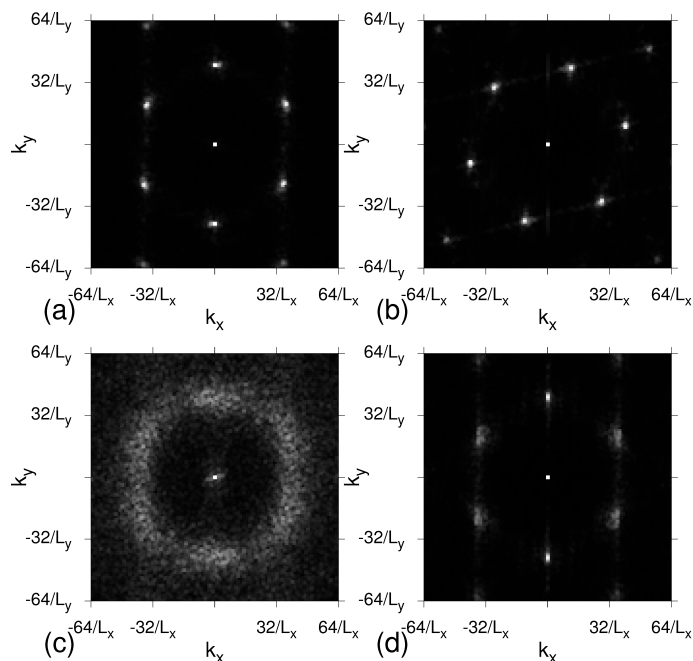


**Fig. 3** The structure factor  $S(\mathbf{k})$  for the four phases in Fig. 2. (a) The jammed phase I at  $F_D = 0.15$  has triangular ordering. (b) The phase separated state II at  $F_D = 0.75$  has triangular ordering. (c) The disordered flow phase III at  $F_D = 3.0$  shows a ring shape indicating liquid ordering. (d) The laning phase IV at  $F_D = 6.5$  has a smectic character with weak triangular ordering.

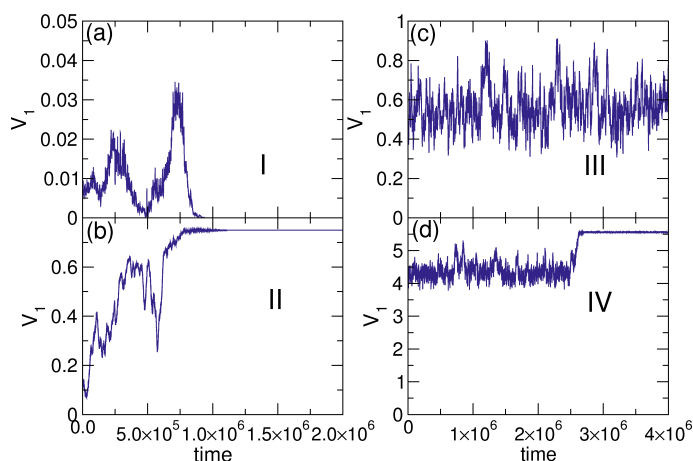


**Fig. 4** The instantaneous velocity  $V_1$  per disk vs time for species 1 for the system in Fig. 1 at  $\phi = 0.848$ . (a) Phase I at  $F_D = 0.15$ , where  $V_1$  goes to zero. (b) Phase II at  $F_D = 0.75$ , where  $V_1$  saturates to a fluctuation-free flowing state with  $V_1 = 0.75$ . (c) Phase III at  $F_D = 1.5$ , where the system remains in a strongly fluctuating state with  $\langle V_1 \rangle = 0.56$ . (d) Phase IV at  $F_D = 5.57$ , where the system is initially in a fluctuating state and organizes at later times into a fluctuation-free flowing state with  $V_1 = 5.57$ .

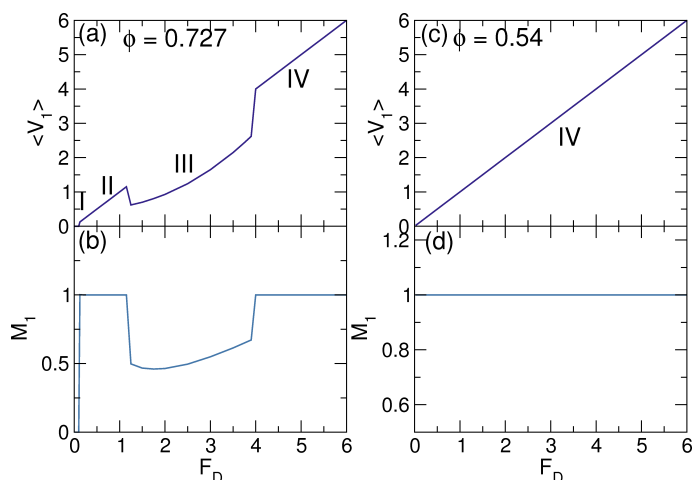


**Fig. 5** (a)  $\langle V_1 \rangle$  vs  $F_D$  for a system with  $N_1 = N_2 = 0.5N_d$  at  $\phi = 0.727$ . (b) The corresponding mobility  $M_1 = \langle V_1 \rangle / F_D$  vs  $F_D$  shows that the I-II and III-IV transitions are shifted to lower values of  $F_D$  compared to the  $\phi = 0.848$  system. (c)  $\langle V_1 \rangle$  and (d) the mobility  $M_1$  vs  $F_D$  for a system with  $\phi = 0.54$ , where the disks are always in phase IV, the velocity-force curve is linear, and  $M_1 = 1$ .

state with  $V_1 = 0.75$ . This corresponds to the formation of the phase separated state, where  $V_2 = -0.75$ . The absence of fluctuations in  $V_1$  and the fact that  $V_1 = F_D$  indicate that the disks are in a completely free flow state and that disk-disk collisions no longer occur. In Fig. 4(c) for phase III at  $F_D = 1.5$ ,  $V_1$  strongly fluctuates between  $V_1 = 0.4$  and  $V_1 = 0.9$ , and the average velocity  $\langle V_1 \rangle = 0.56$  is almost three times smaller than the free flow value of  $\langle V_1 \rangle = 1.5$ . In this phase, the velocity continues to fluctuate out to the longest simulation times we consider, and the strong fluctuations indicate that there are continuous disk-disk collisions that impede the flow of the disks in both directions. Figure 4(d) shows phase IV flow at  $F_D = 5.57$ , where the system is initially in a fluctuating flow phase similar to phase III, but organizes at later times into a non-fluctuating free flow state where all disk-disk collisions are lost.

We investigate the evolution of the phases as a function of  $\phi$  and find that for decreasing  $\phi$  the III-IV transition drops to lower values of  $F_D$ . In Fig. 5(a) we plot  $\langle V_1 \rangle$  versus  $F_D$  for the system in Fig. 1 at  $\phi = 0.727$ , while Fig. 5(b) shows the corresponding mobility  $M_1 = \langle V_1 \rangle / F_D$  versus  $F_D$ . The I-II transition has dropped to  $F_D = 0.1$  and the mobility in phase I is  $M_1 = 0$ . The II-III transition occurs at roughly the same value of  $F_D$  as in the  $\phi = 0.848$  system, but the III-IV transition drops to  $F_D = 4.0$ . When the system is in free flow in phases II and IV,  $M_1 = 1$ , but the mobility is substantially reduced in the disordered flow phase III. In Fig. 5(c,d) we plot  $\langle V_1 \rangle$  and the mobility  $M_1$  versus  $F_D$  for a sample with  $\phi = 0.54$ , where the disks always organize into phase IV flow, the velocity-force

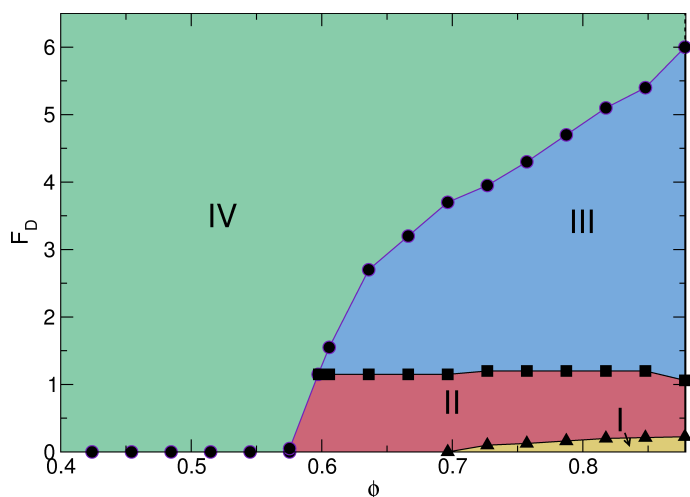


**Fig. 6** Dynamic phase diagram as a function of  $F_D$  vs  $\phi$ . I: jammed phase; II: phase separated state; III: disordered flow phase; IV: laning phase. For  $\phi < 0.55$  the system is always in phase IV, while phase III grows in extent with increasing  $\phi$  for  $\phi > 0.55$ .

curve is linear, and  $M_1 = 1$ .

By conducting a series of simulations we map the evolution of the different phases as a function of  $F_D$  vs  $\phi$ , as shown in the dynamic phase diagram in Fig. 6. For  $\phi > 0.55$ , phases II, III, and IV all occur, while for  $\phi < 0.55$  only phase IV is present. For  $\phi > 0.55$ , the extent of phase III grows with increasing  $\phi$ , and we only observe region I for  $\phi > 0.7$ . The II-III transition occurs at roughly the same value of  $F_D$  as  $\phi$  varies. The minimum value of  $\phi = 0.55$  at which phases II and III first appear may be related to a contact percolation transition. In compressional simulations of 2D monodisperse frictionless disks, Shen *et al.*<sup>38</sup> found a contact percolation transition at  $\phi_p = 0.549$  and argued that this transition is connected to the onset of a non-trivial mechanical response or stress in the system. Several of the phase transitions we observe have similarities to the irreversible-reversible transition observed in periodically sheared disk suspensions, where the system can transition from an irreversible fluctuating state where collisions occur to a reversible state where collisions are lost<sup>37,39</sup>. In our system, in phases II and IV the collisions are lost, while phase III would correspond to an irreversible state. Additionally, the jammed phase can also be viewed as an absorbed state since all fluctuations are lost, even though the particles are now all in contact.

#### 4 Varied Species Ratios and Driving Force Ratios

We have also considered different ratios of  $N_1$  to  $N_2$  and find that the same general phases appear. In Fig. 7(a) we plot

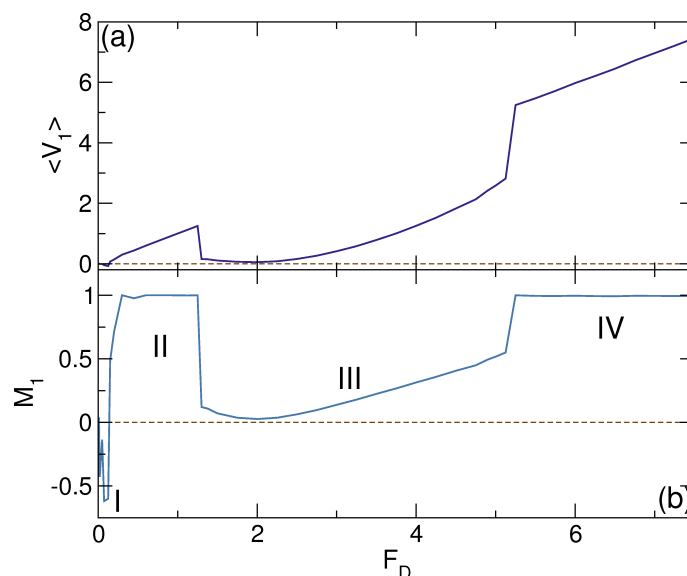


**Fig. 7** (a)  $\langle V_1 \rangle$  vs  $F_D$  for a sample with  $\phi = 0.848$  in which  $N_1 = 0.2N_d$  and  $N_2 = 0.8N_d$ . (b) The corresponding mobility  $M_1$  vs  $F_D$ . Here  $M_1 = 1.0$  in phases II and IV, but there is a portion of phase III for which the mobility is nearly zero. Phase I is no longer a jammed phase with  $\langle V_1 \rangle = 0$ . Instead, a rigid cluster forms that drifts in the  $-x$  direction, producing a negative mobility.

$\langle V_1 \rangle$  versus  $F_D$  for a system with  $\phi = 0.848$ ,  $N_1 = 0.2N_d$ , and  $N_2 = 0.8N_d$ , while Fig. 7(b) shows the corresponding mobility  $M_1$  versus  $F_D$ . Here the same four phases arise and the overall shape of the curves is similar to that of the  $N_1 = N_2 = 0.5N_d$  system shown in Fig. 1; however, in phase III the average mobility drops nearly to zero since the additional collisions suppress the flow of the disks in the  $+x$  direction. In phases II and IV,  $M_1 = 1$ , indicating that the system can still organize into a collisionless state where the disks undergo free flow motion. A notable difference is that for phase I in the  $N_1 = 0.2N_d$  sample, the mobility  $M_1$  is negative. The jammed phase I for the  $N_1 = 0.5N_d$  sample has  $\langle V_1 \rangle = 0$ , but in the  $N_1 = 0.2N_d$  sample, the jammed state consists of a rigid solid that translates in the  $-x$  direction since  $N_2 > N_1$ . In general, for any ratio other than  $N_1/N_2 = 1$ , the jammed phase I has a net drift in the direction of the majority species. As  $N_1/N_2$  is decreased further, in phases II and IV we always find  $M_1 = 1$ , while for phases I and III the mobility decreases or becomes more negative.

We can also change the ratio of the relative driving force on the two different species. We consider a system with  $N_1 = N_2 = 0.5N_d$  at  $\phi = 0.848$  and vary the value of  $C$  controlling the amplitude of the driving force for species 1, while keeping the drive on species 2 fixed at  $\mathbf{F}_D^i = -F_d \hat{\mathbf{x}}$ . Here  $C$  is chosen in the range  $-1.0 \leq C \leq +1.0$ . The exactly oppositely driven disks in Fig. 1 correspond to the case  $C = +1.0$ . For  $C = 0$ , half of the disks do not couple to the external drive while

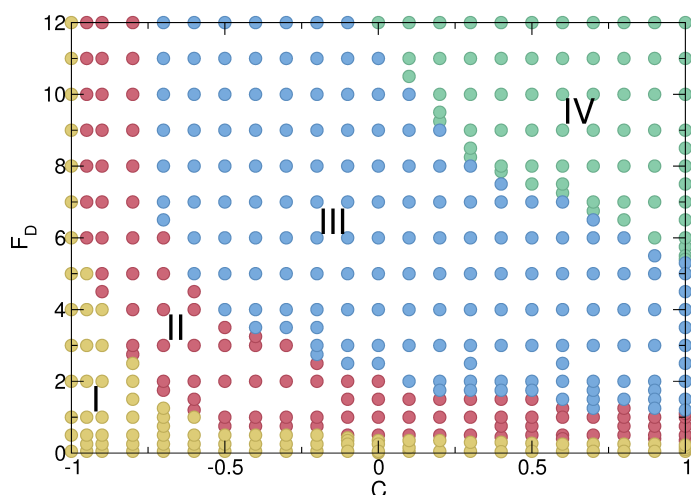


**Fig. 8** Dynamic phase diagram as a function of  $F_D$  vs  $C$ , where  $C$  is the coefficient controlling the amplitude of the driving force for species 1 disks, in a sample with  $N_1 = N_2 = 0.5N_d$  and  $\phi = 0.848$ . The value  $C = 1.0$  corresponds to the case shown in Fig. 1 for exactly oppositely driven particles. Yellow circles: jammed phase I; red circles: phase separated state II; blue circles: disordered flow phase III; and green circles: laning phase IV. At  $C = 0$  where only species 2 couples to the drive, all four phases can still occur.

the other half are driven in the negative  $x$  direction, and for  $-1.0 \leq C < 0$ , both species are driven in the  $-x$  direction with different forces. At  $C = -1.0$ , all the particles are driven in the  $-x$  direction with the same force. In Fig. 8 we show a dynamic phase diagram as a function of  $F_D$  versus  $C$ . All of the phase transitions shift to higher values of  $F_D$  as  $C$  decreases. It is interesting to note that for  $C = 0$ , where only species 2 is driven, all four dynamic phases still occur.

In Fig. 9(a) we plot the instantaneous disk velocities  $V_1$  and  $V_2$  versus time for  $C = 0$  and  $F_D = 1.0$ . Here, species 1 is not driven. The system organizes into phase II as indicated by the transition to  $V_1 = 0$  and  $V_2 = -1.0$ . The velocities rapidly approach the phase II values at short times, but significant velocity fluctuations persist and appear as jumps in both  $V_1$  and  $V_2$  in the transient fluctuating state. In Fig. 9(b), the corresponding  $P_6$  versus  $F_D$  for all the disks shows that the large fluctuations in  $V_{1,2}$  correlate with drops in  $P_6$ , and that when the system fully settles into phase II flow,  $P_6$  saturates to  $P_6 = 0.925$ , indicating mostly triangular ordering. In Fig. 10(a) we show the disk configurations and trajectories in the phase II flow for the  $C = 0$  system in Fig. 9(a). The disks phase separate into an immobile triangular packing surrounded by a moving triangular lattice. At high drives for  $C = 0$ , a laning phase IV appears where half of the lanes are immobile and the other half are moving.

The jammed phase I at  $C = 0$  consists of a moving solid drifting in the  $-x$ -direction, as illustrated in Fig. 9(c) where

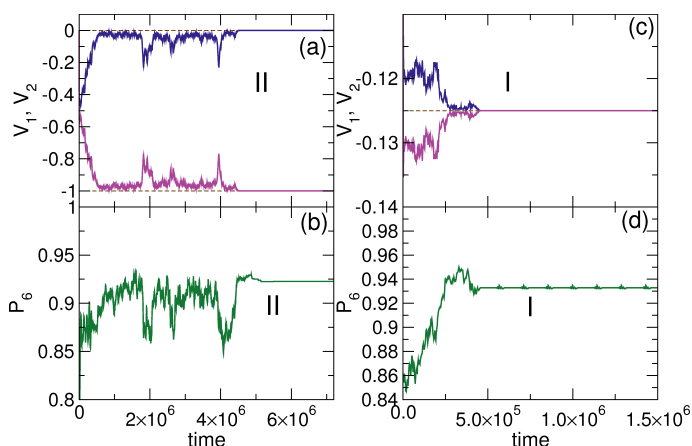


**Fig. 9** A sample from Fig. 8 with  $C = 0$  and  $F_D = 1.0$ . (a) The instantaneous velocity per disk  $V_1$  vs time in simulation time steps (upper blue curve) for the non-driven disks and the corresponding  $V_2$  vs time for the disks driven in the  $-x$  direction. Here the system organizes into phase II flow with  $V_1 = 0$  and  $V_2 = -F_D = -1.0$ . (b)  $P_6$  vs time for all the disks in the same system showing the transition into phase II. (c)  $V_1$  and  $V_2$  vs time for the same system at  $F_D = 0.25$  and  $C = 0$ . The disks organize into phase I where both species become locked together and move at  $V_1 = V_2 = -0.125 = F_D/2$ . (d) The corresponding  $P_6$  vs time curve shows that the system organizes into a mostly triangular state at the transition to phase I.

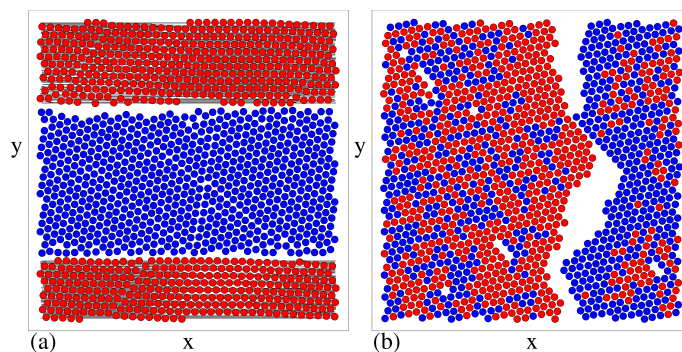


**Fig. 10** The disk configurations for the system in Fig. 9 with  $C = 0$ . The blue disks (species 1) are not driven and the red disks (species 2) are driven in the  $-x$  direction. (a) The phase separated state II for the system in Fig. 9(a,b) at  $F_D = 1.0$ . The black lines are the disk trajectories indicating that the system has phase separated into moving and non-moving spatial regions. (b) The jammed state I at  $F_D = 0.25$  from Fig. 9(c,d) where the entire system is moving in the negative  $x$ -direction.

we plot  $V_1$  and  $V_2$  versus time at  $F_D = 0.25$ . Here the velocities of both disk species converge to  $V_1 = V_2 = -0.125 = -F_D/2$  in phase I since the non-driven disks reduce the velocity of the driven disks to half of its free-flow value. Figure 9(d) shows the corresponding  $P_6$  versus time, where at the transition into phase I,  $P_6 = 0.93$  indicating the formation of a triangular drifting solid. In Fig. 10(b) we show the disk configurations in phase I for the system in Fig. 9(c), where the driven disks drag the non-driven disks.

Phases I and II persist for  $-1.0 < C < 0.0$  in the range of  $F_D$  that we have investigated, and at  $C = -1$  all the disks move in unison. The fact that these phases can occur over a range of relative drives indicates that such phases may be general to other systems in which the particles are not exactly oppositely driven but have differences in their relative driving. These differences could arise for particles with different drag coefficients, different coupling to a substrate, different amounts of charge, different shapes, and so forth. Such effects could also be realized for active matter systems where one species couples to an external drift force or where only one species is active. There are already examples of mixtures of active and non-active particles that undergo phase separation<sup>40</sup>. Another interesting feature of this system at  $C = 0$  is that certain regimes such as phase II flow exhibit a time dependent resistance. When the drive is initially applied, the sample enters a high resistance state in which many collisions occur, but over time the disks approach a low resistance state as the number of collisions are reduced. This suggests that if finite temperature were included, then when the drive is shut off there would be a finite time during which the memory of the low-resistance organized state is preserved. Such a system would have features similar to those of a memristor<sup>41</sup>.

## 5 Summary

We have numerically investigated a two-dimensional disk system in which two disk species are driven in opposite directions. We characterize the system by measuring the average velocity of one disk species as a function of drive to create a velocity-force curve analogous to what is observed in driven systems with quenched disorder. The density  $\phi$  is the total area coverage of the disks, and for  $\phi > 0.55$  we identify four dynamical phases: a crystalline jammed phase I, a fully phase separated state II where the particles are not in contact but exhibit six-fold ordering, a strongly fluctuating liquid phase III where continuous collisions are occurring, and a laning phase IV or smectic state where collisions are absent. The transitions between these different phases are associated with jumps or dips in the velocity-force curves and the differential mobility along with global changes in the disk configurations. At the transition into phase III we find negative differential mobility. The transitions also correlate with jumps in the amount of six-

fold ordering. For  $\phi < 0.55$ , the system always organizes into the laning phase IV and the velocity-force curves are linear. We vary the relative driving forces on the two species, and consider the case where one species is driven while the other species does not couple to the drive as well as the case where both species are driven in the same direction with different relative forces. We find that the same four driven phases found for the oppositely driven case still occur. By measuring the instantaneous disk velocities, we find that in phases II and IV, the disks organize into a freely flowing state in which disk-disk collisions no longer occur. We discuss how the transitions into phases II and IV may be related to the irreversible-reversible transitions recently observed for periodically sheared colloidal or granular systems, which organize to a state where the collisions between particles are lost.

## 6 Acknowledgements

This work was carried out under the auspices of the NNSA of the U.S. DoE at LANL under Contract No. DE-AC52-06NA25396.

## References

- 1 C. Reichhardt and C.J.O. Reichhardt, *Rep. Prog. Phys.*, 2017, **80**, 026501.
- 2 S. Bhattacharya and M. J. Higgins, *Phys. Rev. Lett.*, 1993, **70**, 2617.
- 3 A. E. Koshelev and V. M. Vinokur, *Phys. Rev. Lett.*, 1994, **73**, 3580.
- 4 C.J. Olson, C. Reichhardt, and F. Nori, *Phys. Rev. Lett.*, 1998, **81**, 3757.
- 5 F.I.B. Williams, P.A. Wright, R.G. Clark, E.Y. Andrei, G. Deville, D.C. Glattli, O. Probst, B. Etienne, C. Dorin, C.T. Foxon, and J.J. Harris, *Phys. Rev. Lett.*, 1991, **66**, 3285.
- 6 A. Pertsinidis and X.S. Ling, *Phys. Rev. Lett.*, 2008, **100**, 028304.
- 7 P. Tierno, *Phys. Rev. Lett.*, 2012, **109**, 198304.
- 8 T. Bohlein, J. Mikhael, and C. Bechinger, *Nature Mater.*, 2012, **11**, 126.
- 9 C. Reichhardt and C.J.O. Reichhardt, *Phys. Rev. E*, 2012, **85**, 051401.
- 10 D. McDermott, J. Amelang, C.J.O. Reichhardt, and C. Reichhardt, *Phys. Rev. E*, 2013, **88**, 062301.
- 11 O.M. Braun, T. Dauxois, M.V. Paliy, and M. Peyrard, *Phys. Rev. Lett.*, 1997, **78**, 1295.
- 12 A. Vanossi, N. Manini, M. Urbakh, S. Zapperi, and E. Tosatti, *Rev. Mod. Phys.*, 2013, **85**, 529.
- 13 P. Le Doussal and T. Giamarchi, *Phys. Rev. B*, 1998, **57**, 11356.
- 14 L. Balents, M.C. Marchetti, and L. Radzihovsky, *Phys. Rev. B*, 1998, **57**, 7705.
- 15 F. Pardo, F. de la Cruz, P.L. Gammel, E. Bucher, and D.J. Bishop, *Nature (London)*, 1998, **396**, 348.
- 16 A. Kolton, D. Domínguez, and N. Grønbech-Jensen, *Phys. Rev. Lett.*, 1999, **83**, 3061.
- 17 C. Reichhardt, C. J. Olson, and F. Nori, *Phys. Rev. Lett.*, 1997, **78**, 2648.
- 18 J. Gutierrez, A. V. Silhanek, J. Van de Vondel, W. Gillijns, and V. Moshchalkov, *Phys. Rev. B*, 2009, **80**, 140514.
- 19 C. Reichhardt and C.J.O. Reichhardt, *Phys. Rev. B*, 2008, **78**, 224511.
- 20 C. Reichhardt and C.J.O. Reichhardt, *Phys. Rev. E*, 2006, **74**, 011403.
- 21 R. Candelier and O. Dauchot, *Phys. Rev. E*, 2010, **81**, 011304.
- 22 J. Dzubiella, G.P. Hoffmann, and H. Löwen, *Phys. Rev. E*, 2002, **65**, 021402.
- 23 R.R. Netz, *Europhys. Lett.*, 2003, **63**, 616.

- 
- 24 T. Glanz and H. Löwen, *J. Phys.: Condens. Matter*, 2012, **24**, 464114.
  - 25 K. Klymko, P.L. Geissler, and S. Whitlam, *Phys. Rev. E*, 2016, **94**, 022608.
  - 26 E.M. Foulaadvand and B. Aghaee, *Eur. Phys. J. E*, 2016, **39**, 37.
  - 27 C.W. Wächtler, F. Kogler, and S.H.L. Klapp, *Phys. Rev. E*, 2016, **94**, 052603.
  - 28 A. Poncet, O. Bénichou, V. Démery, and G. Oshanin, *Phys. Rev. Lett.*, 2017, **118**, 118002.
  - 29 T. Vissers, A. Wysocki, M. Rex, H. Löwen, C.P. Royall, A. Imhof, and A. van Blaaderen, *Soft Matter*, 2011, **7**, 2352.
  - 30 K. Sütterlin, A. Wysocki, A. Ivlev, C. Räth, H. Thomas, M. Rubin-Zuzic, W. Goedheer, V. Fortov, A. Lipaev, V. Molotkov, O. Petrov, G. Morfill, and H. Löwen, *Phys. Rev. Lett.*, 2009, **102**, 085003.
  - 31 B. Schmittmann, K. Hwang, and R.K.P. Zia, *Europhys. Lett.*, 1992, **19**, 19.
  - 32 M. Ikeda, H. Wada, and H. Hayakawa, *EPL*, 2012, **99**, 68005.
  - 33 D. Helbing, I.J. Farkas, and T. Vicsek, *Phys. Rev. Lett.*, 2000, **84**, 1240.
  - 34 D. Helbing, *Rev. Mod. Phys.*, 2001, **73**, 1067.
  - 35 C. Reichhardt and C.J.O. Reichhardt, *Soft Matter*, 2014, **10**, 2932.
  - 36 H. Hinrichsen, *Adv. Phys.*, 2000, **49**, 815.
  - 37 L. Corté, P.M. Chaikin, J.P. Gollub, and D.J. Pine, *Nature Phys.*, 2008, **4**, 420.
  - 38 T. Shen, C.S. O'Hern, and M.D. Shattuck, *Phys. Rev. E*, 2012, **85**, 011308.
  - 39 C.F. Schreck, R.S. Hoy, M.D. Shattuck, and C.S. O'Hern, *Phys. Rev. E*, 2013, **88**, 052205.
  - 40 C. Bechinger, R. Di Leonardo, H. Löwen, C. Reichhardt, G. Volpe, and G. Volpe, *Rev. Mod. Phys.*, 2016, **88**, 045006.
  - 41 L.O. Chua, *Appl. Phys. A*, 2011, **102**, 765.